Available online at www.sciencedirect.com
SCIENCE DIRECT®
International Journal of Heat and Fluid Flow 25 (2004) 331–340
International Journal of HEAT AND FLUID FLOW
www.elsevier.com/locate/ijhff

Scaling law of fine scale eddies in turbulent channel flows up to $Re_\tau = 800$

M. Tanahashi *, S.-J. Kang, T. Miyamoto, S. Shiokawa, T. Miyauchi

Department of Mechanical and Aerospace Engineering, Tokyo Institute of Technology, 2-12-1 Ookayama, Meguro-ku, Tokyo 152-8552, Japan

Abstract

To clarify the scaling law of fine scale eddies in turbulent channel flows, direct numerical simulations are conducted for $Re_\tau = 180$, 400 and 800. The diameter and the maximum azimuthal velocity of coherent fine scale eddies can be scaled by Kolmogorov microscale (η) and Kolmogorov velocity (u_k). The most expected diameter and maximum azimuthal velocity are 8–10η and 1.2–2.0u_k, respectively. Near the wall, the most expected diameter increases to 10η from 8η and the most expected maximum azimuthal velocity increases to 2.0u_k from 1.2u_k. Strain rates at the center of the coherent fine scale eddies are small compared with the mean strain rate of the whole flow field. The strain rates acting on the fine scale eddies away from the wall coincide with those in homogeneous isotropic turbulence and turbulent mixing layer. However, relatively large strain rates are acting on the near-wall coherent fine scale eddies. The most expected angle between the intermediate eigenvector and the rotating axis of the fine scale eddy is about 15–17°, which is independent of the turbulent flow fields. The probability that coherent fine scale eddies exist in low-speed streaks is higher than that in high-speed streaks. Large scale structures of wall turbulence are visualized by showing spatial distributions of central axes of coherent fine scale eddies.
© 2004 Elsevier Inc. All rights reserved.

PACS: 02.70.Hm; 47.27.Eq; 47.27.Jv; 83.50.Ha
Keywords: Coherent structure; Coherent fine scale eddy; Direct numerical simulation; Turbulent channel flow; Wall turbulence

1. Introduction

Theoretical description of intermittent character in small scale motion has been one of the most important subjects in turbulence research. Theorists have made efforts to establish theories of fine scale structure of turbulence by assuming various types of vortices as fine scale structure (Corrsin, 1962; Lundgren, 1982; Pullin and Saffiman, 1993; Tennekes, 1968; Townsend, 1951). Most of them are based on an assumption that many tube-like vortices are embedded in turbulence randomly. Owing to direct numerical simulations (DNS) of turbulence, it has been found that turbulence is composed of universal fine scale eddies, which are verified in homogeneous isotropic turbulence (Jimenez et al., 1993; Tanahashi et al., 1999a), turbulent mixing layer (Tanahashi et al., 2001) and turbulent channel flow (Tanahashi et al., 1999c). In turbulent mixing layers, large scale structures which were found by Brown and Roshko (1974) are composed of many coherent fine scale eddies (Tanahashi et al., 2001). In turbulent channel flows, well-known streamwise vortices possess the same feature as the coherent fine scale eddies (Tanahashi et al., 1999b,c). The characteristics of these eddies in low Reynolds number flows can be scaled by the Kolmogorov microscale (η) and rms of velocity fluctuation ($u_{\rm rms}$), and the most expected diameter and maximum azimuthal velocity are about 8η and 0.5–1.0$u_{\rm rms}$, respectively. Recent study in homogeneous isotropic turbulence up to $Re_\lambda \approx 220$ has revealed the exact scaling of these coherent fine scale eddies (Miyauchi et al., 2002). The diameter and the maximum azimuthal velocity are scaled by η and the Kolmogorov velocity (u_k), respectively. Similar to the results obtained in low Re_λ cases (Jimenez et al., 1993; Tanahashi et al., 1999a), the most expected diameter is 8η even for highest Re_λ. On the other hand, the most expected value of the

* Corresponding author. Tel.: +81-35-734-3181; fax: +81-35-734-3982.
E-mail address: mtanahas@mes.titech.ac.jp (M. Tanahashi).

0142-727X/$ - see front matter © 2004 Elsevier Inc. All rights reserved.
doi:10.1016/j.ijheatfluidflow.2004.02.016

Table 1
Numerical parameters for DNS of turbulent channel flows

Re_τ	Re	$L_x \times L_y \times L_z$	$N_x \times N_y \times N_z$	Δ_x^+	Δ_y^+	Δ_z^+
180	3276	$4\pi\delta \times 2\delta \times 2\pi\delta$	$192\times193\times160$	11.781	0.433–4.664	7.069
400	8200	$2\pi\delta \times 2\delta \times \pi\delta$	$256\times385\times192$	9.817	0.479–5.183	6.544
800	17,760	$2\pi\delta \times 2\delta \times \pi\delta$	$512\times769\times384$	9.817	0.479–5.183	6.544

maximum azimuthal velocity can be scaled by u_k instead of $u_{\rm rms}$ and is $1.2u_k$ for all Re_λ. It should be noted that the azimuthal velocity of intense fine scale eddies of which diameter is about 8η remains to be scaled by $u_{\rm rms}$ and reaches to 3–4$u_{\rm rms}$ even at high Re_λ.

From previous studies for homogeneous isotropic turbulence and turbulent mixing layer, it has been reported that the most expected eigenvalue ratio of strain rate is −5:1:4 at the centers of coherent fine scale eddies, and the eigenvector of the minimum eigenvalue tends to be perpendicular to the rotating axis of the coherent fine scale eddy and the angle between the rotating axis and the eigenvector of intermediate eigenvalue is less than 45° for about 70% of the fine scale eddy (Miyauchi et al., 2002; Tanahashi et al., 2001). Blackburn et al. (1996) have reported that the eigenvector of the intermediate eigenvalue shows a tendency to be parallel to the vorticity vector in the near-wall region of turbulent channel flow with $Re_\tau = 395$. Tanahashi et al. (1999c) have investigated the alignment and the ratio of the eigenvalues at the center of coherent fine scale eddy for low Reynolds number cases.

Over the past few decades, a number of studies have been conducted on relation between a low-speed streak and the structure of wall turbulence. The average length of a low-speed streak associated with a hairpin vortex is about two to three hundred wall units in low-Reynolds number channel flow (Kim, 1983). The most widely observed coherent structures in the wall layer are streaks: elongated regions of high- and low-speed fluid alternating in the spanwise direction (Choi et al., 1994). The generation of the quasi-streamwise vortices is associated with changes in the shape of a low-speed streak surface (Soldati, 2000). However, there are few studies about quantitative relations between low-speed streaks and fine scale eddies. For identification of vortical structures in turbulent flow, a considerable number of investigations have been reported. For example, Tanaka and Kida (1993) have used $\nabla^2 p$ to represent streamwise vortices in homogeneous shear flows. $\nabla^2 p$ corresponds to twice the second invariant Q of the velocity gradient tensor. Jeong et al. (1997) and Blackburn et al. (1996) have used λ_2 definition and Δ definition to investigate vortical structure near the wall. However, all of these identification methods depend on the threshold value of the variables.

In this study, direct numerical simulations of turbulent channel flows up to $Re_\tau = 800$ are conducted. From these DNS data, the scaling law of fine scale eddies near the wall is investigated, and large and small scale coherent structures of wall turbulence are visualized by showing spatial distributions of the axes of coherent fine scale eddies.

2. Turbulent statistics

In this study, direct numerical simulations of turbulent channel flows up to $Re_\tau = 800$, where Re_τ is the Reynolds number based on the friction velocity (u_τ) and the channel half width (δ), were conducted by solving incompressible Navier–Stokes equations and continuity equation. The computational domain size (L_x, L_y, L_z), the number of grid points (N_x, N_y, N_z) and spatial resolution ($\Delta_x^+, \Delta_y^+, \Delta_z^+$) are given in Table 1. Spectral methods are used in the streamwise (x) and spanwise (z) directions, and a fourth-order central finite difference scheme is used in the transverse (y) direction. This DNS code has been verified by comparing with the result of Kim et al. (1987). Computations were carried out until the turbulent flow field attains statistical steady state.

Fig. 1 shows the mean velocity profiles for $Re_\tau = 180$, 400 and 800, where the wall-normal coordinate is given in wall units and the mean velocity is normalized by the friction velocity (u_τ). The solid and dashed lines represent the linear and the log law, respectively. All curves in $y^+ < 5$ are independent of Re_τ. The curves in $y^+ > 20$ both for $Re_\tau = 400$ and 800 coincide with the dashed line, but the curve of $Re_\tau = 180$ shifts upward from it. Moreover, it should be noted that the wake region is clearly distinguishable for $Re_\tau = 800$. Root-mean-square velocity fluctuations normalized by u_τ are shown in Fig. 2. These peak values slightly increase with the increase

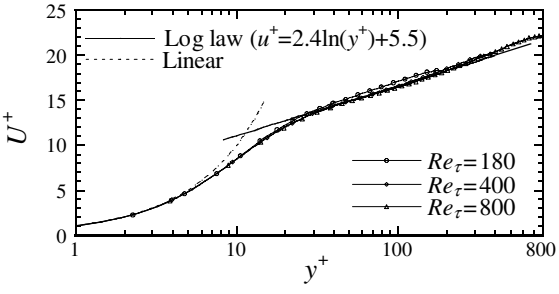

Fig. 1. Mean velocity profiles for $Re_\tau = 180$, 400 and 800.

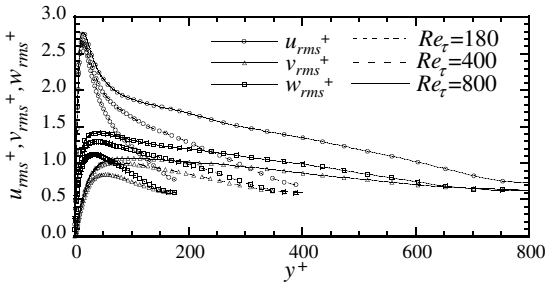

Fig. 2. Root-mean-square velocity fluctuations for $Re_\tau = 180$, 400 and 800.

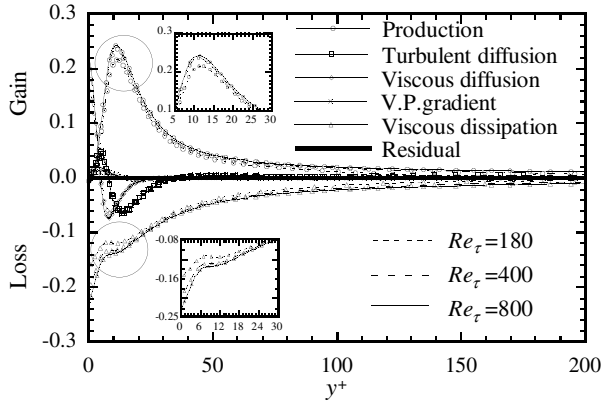

Fig. 3. The budget of the transport equation for the turbulent energy for $Re_\tau = 180$, 400 and 800.

of Re_τ. Especially, wall-normal and spanwise components highly depend on Re_τ and positions of the peak values are slightly away from the wall as Re_τ increases.

Fig. 3 shows the budget of the turbulent kinetic energy for all Reynolds numbers in wall coordinates. The absolute values of the production and the dissipation terms for $Re_\tau = 180$ are smaller than the results for $Re_\tau = 400$ and 800, but the ratio of these terms is independent of Re_τ as shown by Moser et al. (1999). We could verify that the budget of the transport equation for the Reynolds stress also shows the similar trend with the budget of the turbulent kinetic energy and these residuals are almost zero.

3. Fine scale eddies of high Reynolds number turbulent channel flow

There are a lot of methods for identification of vortical structures in turbulent flows. High vorticity or enstrophy regions are the simplest method to visualize the vortical structures. In previous works related to fine scale structures in homogeneous isotropic turbulence, high vorticity regions have been used to identify the intermittent fine scale structure of turbulence (Jimenez et al., 1993; She et al., 1990). However, high vorticity regions may represent tube-like and sheet-like structures simultaneously. For the case with a strong mean shear like the flows near the wall or center of free shear flows, employment of high vorticity or enstrophy regions fails to represent coherent eddies. For visualization purposes, iso-surfaces of the second invariant of the velocity gradient tensor are shown for $Re_\tau = 800$ in Fig. 4. The region visualized is the lower half of the calculation domain. The second invariant of the velocity gradient tensor is given by $Q(= (W_{ij}W_{ij} - S_{ij}S_{ij})/2)$, where $S_{ij}(= (\partial u_i/\partial x_j + \partial u_j/\partial x_i)/2)$ and $W_{ij}(= (\partial u_i/\partial x_j - \partial u_j/\partial x_i)/2)$ are the symmetric and asymmetric parts of the velocity gradient tensor $A_{ij}(= \partial u_i/\partial x_j = S_{ij} + W_{ij})$. Fig. 4 indicates that there are a lot of tube-like structures in turbulent channel flow similar to homogeneous isotropic turbulence and turbulent mixing layer. In turbulent channel flow, streamwise vortices near the wall and hairpin-like vortices (Zhou et al., 1999) can be visualized by the positive Q region. Jeong et al. (1997) and Blackburn et al. (1996) have used λ_2 definition and Δ definition to investigate vortical structure near the wall. However, all of the visualizations including Fig. 4 depend on the threshold value of the variables. Therefore, in this study, fine scale eddies are brought out without any threshold by using a new identification scheme based on local flow pattern which was used in our previous studies on homogeneous isotropic turbulence (Tanahashi et al., 1999a). The identification scheme consists of the following steps:

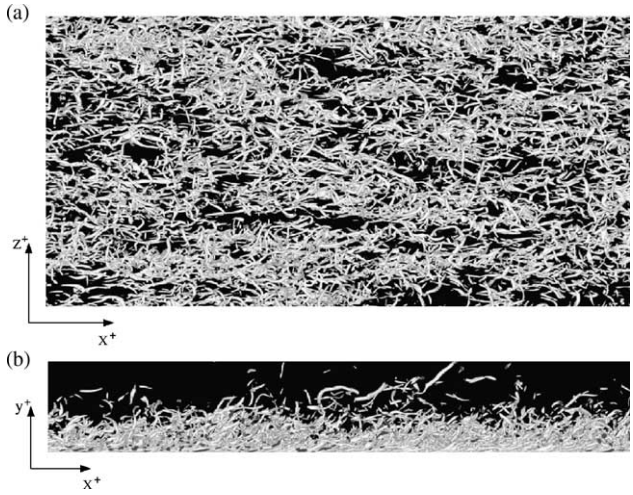

Fig. 4. Iso-surfaces of the second invariant of the velocity gradient tensor for $Re_\tau = 800$ ($Q = 10$, domain size: $l_x^+ \times l_y^+ \times l_z^+ = 5026 \times 800 \times 2513$): (a) top view, (b) side view.

- Evaluation of Q at each collocation point from the results of DNS.
- Probability of existence of positive maxima of Q near the collocation points is evaluated at each collocation point from the Q distribution. The case that a

maximum of Q coincides with a collocation point is very rare, so it is necessary to define probability on collocation points.

- Collocation points with high possibility of existence are selected to survey actual maxima of Q. Locations of Q maxima are determined by applying a three dimensional fourth-order Lagrange interpolation to DNS data.
- At the maximum second invariant point, a horizontal plane perpendicular to the vorticity vector is defined and a cylindrical coordinate system with the maximum point as the origin is considered. The velocity vectors are projected on this coordinate and mean azimuthal velocity is calculated.
- A point that has minimum variance of azimuthal velocity is surveyed near the maximum point. In this process, cylindrical coordinate system is always renewed around a new searched point.
- Statistical properties are calculated around the points.

From the distribution of Q, two-dimensional sections of fine scale eddies are identified by using the new identification scheme. The section brought out includes a local maximum of Q along the axis of a fine scale eddy and a central point of swirling motion is identified. The radius of the coherent fine scale eddy can be identified by the location of the maximum azimuthal velocity on the plane perpendicular to the vorticity and passing through the $Q_{\max}$ point, thereby negating the need of a threshold.

Fig. 5 shows the probability density functions (pdf) of the diameter and the maximum azimuthal velocity of the fine scale eddies for $Re_\tau = 800$. The diameter and the maximum azimuthal velocity are normalized by η and u_k, which are calculated from mean energy dissipation rate at y^+, where the eddy exists. Both pdfs do not depend on Re_τ (the results for low Re_τ cases are not shown here), whereas they have weak y^+-dependence. Near the wall, the most expected diameter and maximum azimuthal velocity are about 10η and $2.0u_k$, respectively. Leaving from the wall, the most expected diameter and maximum azimuthal velocity become about 8η and $1.2u_k$, which coincide with those in homogeneous isotropic turbulence (Miyauchi et al., 2002). The fine scale eddies near the wall are slightly wider and stronger than those in homogeneous isotropic turbulence.

In addition to the diameter and the maximum azimuthal velocity, the spatial distribution of the axes also shows characteristic feature near the wall. Fig. 6 shows the inclination angles and the tilting angles of the coherent fine scale eddies for $Re_\tau = 800$. The inclination angle (ϕ_y) and the tilting angle (ϕ_z) are defined on the right side of Fig. 6 using the same convention as Jeong et al. (1997). These two angles show strong directional dependence with the decrease of y^+. These features correspond to hairpin-like eddies and streamwise vortices observed near the wall (Adrian et al., 2000; Tanahashi et al., 1999b,c). Fig. 6(a) indicates a strong concentration at $\phi_y \approx 30$–$50°$ near the wall ($10 < y^+ < 200$). The PIV measurements of Adrian et al. (2000) show that x–y plane ($y^+ < 50$–100) patterns of ejection near the wall are consistent with the vortex legs bending and becoming quasi-streamwise vortices, and the inclination angles of the neck and head vary from 15° to 75° (45° is typical). The tilting angle of $\phi_z \approx 90°$ indicates that the centers of the coherent fine scale eddies are distributed in the head of hairpin type vortices (cane vortex, arch vortex, hairpin vortex etc). Note that the directional dependence of the axis is stronger in ϕ_y than in ϕ_z. This result indicates that a large number of the coherent fine scale eddies are distributed in the neck and legs of hairpin type vortices rather than in the head of those. Fig. 6 suggests that directional dependence of the

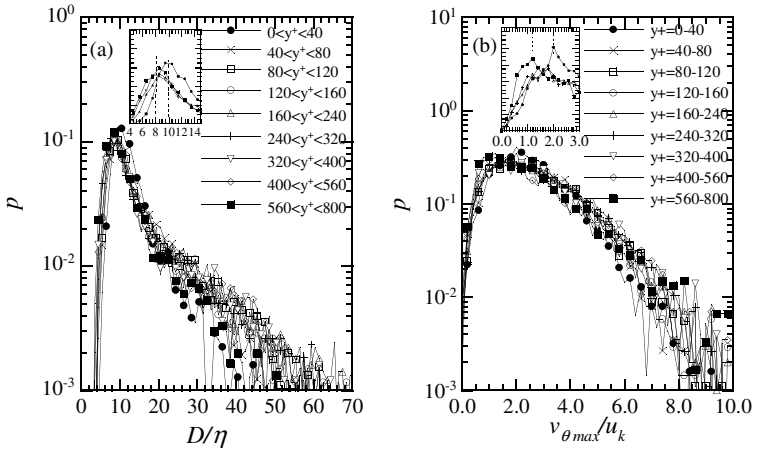

Fig. 5. Probability density functions of diameter (a) and azimuthal velocity (b) of the coherent fine scale eddies for $Re_\tau = 800$.

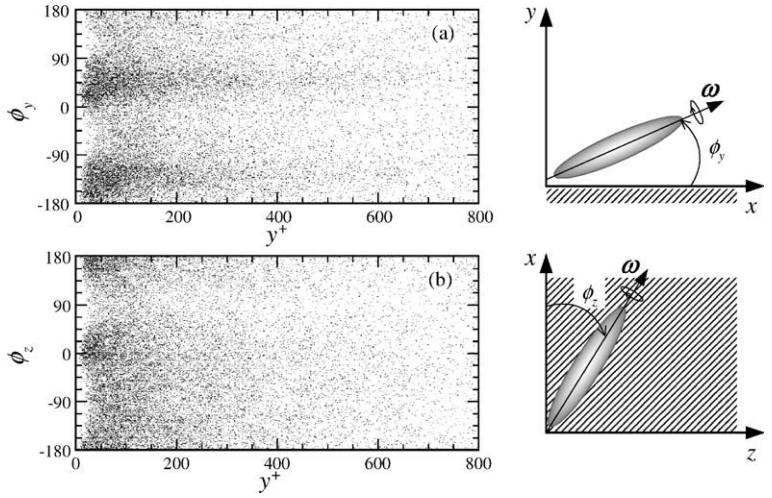

Fig. 6. The inclination angle (a) and the tilting angle (b) of the coherent fine scale eddies ($Re_\tau = 800$).

axis can be observed even for $y^+ \approx 600$. The variance of the diameters becomes relatively small near the wall as shown in Fig. 5(a), and the diameter of almost all coherent fine scale eddies near the wall is about 10η. Therefore, the anisotropy near the wall can be attributed to the smallest coherent fine scale eddies. These results suggest that the anisotropic feature in near-wall turbulence is significantly different from that in free-shear turbulence (Tanahashi et al., 2001) from the viewpoint of the fine scale structure.

4. Coherent fine scale eddies and strain rate field

Strain rate acting on the coherent fine scale eddies is investigated by evaluating the strain rate tensor S_{ij} at the center of the coherent fine scale eddies. The definitions of eigenvalues and eigenvectors of S_{ij} are given by

$$\boldsymbol{S} = \boldsymbol{R}\begin{pmatrix} \alpha & 0 & 0 \\ 0 & \beta & 0 \\ 0 & 0 & \gamma \end{pmatrix}\boldsymbol{R}^{\mathrm{T}}, \quad \boldsymbol{R} = (e_\alpha, e_\beta, e_\gamma), \tag{1}$$

where α, β and γ are the minimum, intermediate and maximum eigenvalues, respectively. The unit eigenvectors corresponding to α, β and γ are represented by e_α, e_β and e_γ. Due to the assumption of incompressibility, relation $\alpha + \beta + \gamma = 0$ ($\alpha \leqslant 0 \leqslant \beta$, $\alpha \leqslant \beta \leqslant \gamma$) holds. Fig. 7 shows the definition of angles between vorticity vector and eigenvectors at the center of a coherent fine scale eddy. Here $\boldsymbol{\omega}$ denotes the vorticity vector at the center of a coherent fine scale eddy, and θ, ψ, and ϕ are defined by the angles between $\boldsymbol{\omega}$ and three unit eigenvectors e_α, e_β and e_γ.

Fig. 8(a) shows pdfs of the eigenvalues calculated in the whole flow field. The eigenvalues are normalized by

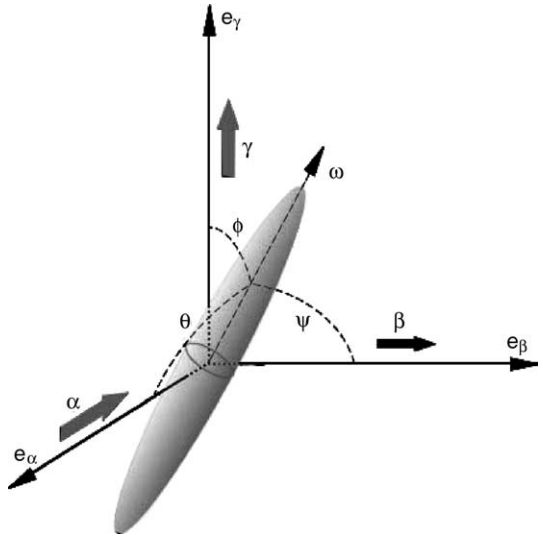

Fig. 7. Definition of angles between a rotating axis and eigenvectors of strain rate tensor.

η and u_k. Near the wall, the pdf of intermediate eigenvalue indicates a sharp peak at about zero, but it skews into the positive portion and the most expected value becomes about $0.06u_k/\eta$ far from the wall. The most expected minimum eigenvalue increases with the increase of distance from the wall, while the most expected maximum eigenvalue decreases. Fig. 8(b) shows pdfs of the eigenvalues evaluated at centers of the coherent fine scale eddies. The eigenvalues in Fig. 8(b) are also normalized by u_k/η as in Fig. 8(a). Pdfs of the eigenvalues near the wall are different from those at the channel center. Near the wall, pdfs of α, β and γ show peaks at about -0.32, 0.04 and 0.27 u_k/η, respectively. At the center of channel, these peak values are -0.25, 0.04 and 0.2 u_k/η, respectively, which coincide with those of homogeneous isotropic turbulence and turbulent mixing

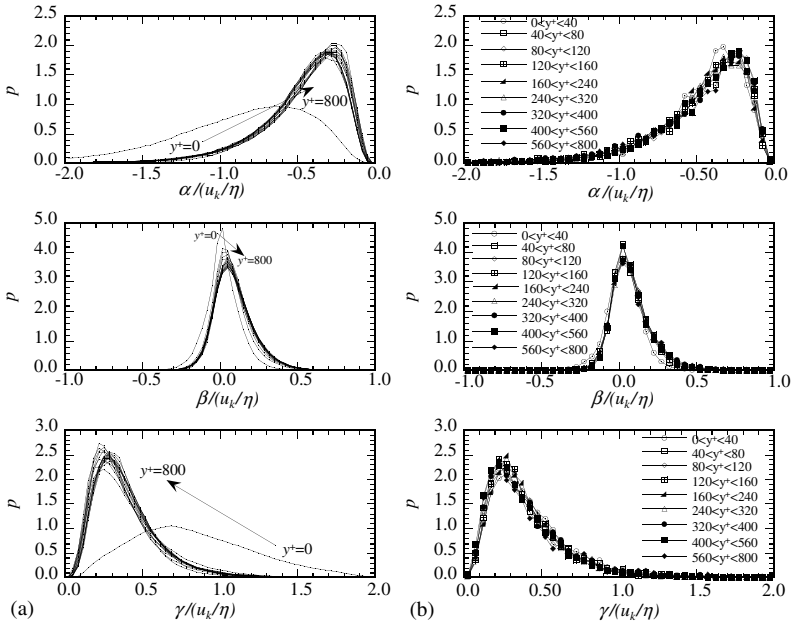

Fig. 8. Probability density functions of eigenvalues of the strain rate tensor for $Re_\tau = 800$: (a) whole flow field (every 20 y^+), (b) at the center of coherent fine scale eddies.

layer. Pdfs of the eigenvalues of strain rate acting on the center of coherent fine scale eddies show a very good agreement with those obtained from the whole flow field except for the near-wall region, but the absolute values of the most expected eigenvalues are smaller than those obtained from the whole flow field. In other words, these results suggest that strain rate acting on the center of coherent fine scale eddies is smaller than that in the mean shear field, which is consistent with the fact that the center of the coherent fine scale eddy is the $Q_{\max}$ point.

To investigate the ratio of eigenvalues at centers of the coherent fine scale eddies, an eigenvalue ratio σ is introduced by $\sigma = (\gamma - \beta)/(\gamma + \beta)$ $(0 \leqslant \sigma \leqslant 3)$. Fig. 9 shows the pdf of the eigenvalue ratio for $Re_\tau = 800$. The peak of pdf increases from about 0.5–0.6 to 0.7 as y^+ decreases. The most expected eigenvalue ratio corresponding to $\sigma = 0.5$–0.6 is $\alpha{:}\beta{:}\gamma = -5{:}1{:}4$ to $\sim -4{:}1{:}3$ from the incompressible constraint. This eigenvalue ratio coincides with that in homogeneous isotropic turbulence and turbulent mixing layer (Tanahashi et al., 2001). Since the eigenvalue ratio shows a peak at $\sigma = 0.7$ near the wall, the most expected eigenvalue ratio becomes $\alpha{:}\beta{:}\gamma = -7{:}1{:}6$. Note that the large compression and stretching are acting on the coherent fine scale eddies in the near-wall region.

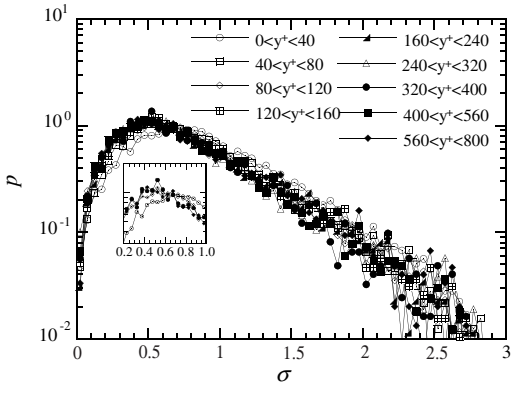

Fig. 9. Probability density functions of eigenvalue ratio at the center of coherent fine scale eddies ($Re_\tau = 800$).

Fig. 10(a) shows pdfs of the angles between the local vorticity vectors and the unit eigenvectors of strain rate in the whole flow field. Near the wall, probabilities of θ, ψ and ϕ show peaks at $\theta = 90°$, $\psi = 0°$ and $\phi = 90°$, respectively. Far from the wall, pdfs of ψ show peak at about 25°, but those of θ and ϕ still peak at about 90°. Pdfs of the angles between the unit eigenvectors and the axes of coherent fine scale eddies are plotted in Fig. 10(b). Pdfs of θ and ϕ show similar trends with those in Fig. 10(a) except for the region near the wall. However, at the center of the coherent fine scale eddies, probabilities of peaks at about 90° are slightly higher than those in the whole flow field. The probability of a peak for θ in the near-wall region is lower than that in the channel center, and pdf of ϕ shows a peak at 73–76° near the wall. In the near-wall region, pdf of ψ sharply increases from zero and gradually decreases after showing peaks at 15–17°. Note that the pdfs peaks in Fig. 10 are not sharp, especially far from the wall, and spread over a small region.

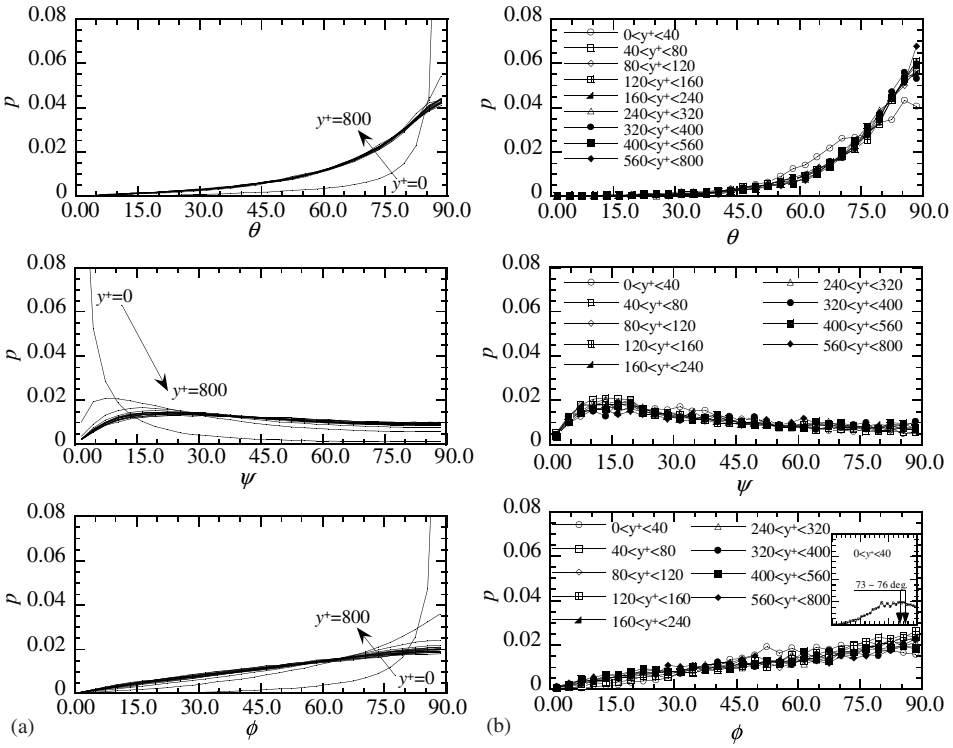

Fig. 10. Probability density functions of the angles between unit eigenvectors of strain rate tensor and vorticity vectors for $Re_\tau = 800$: (a) whole flow field, (b) at the center of coherent fine scale eddies.

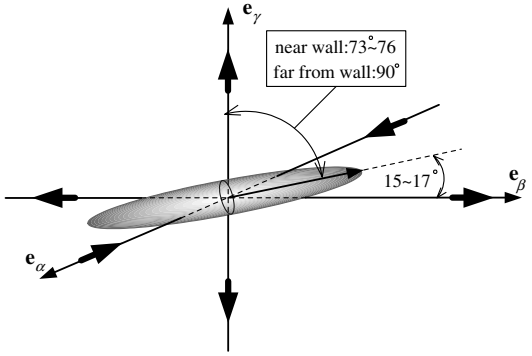

Fig. 11. Schematic of alignment of a coherent fine scale eddy with strain rate field.

From these results, the alignment of a coherent fine scale eddy with the principal strain rates is schematically shown in Fig. 11. The rotating axes of the coherent fine scale eddies are perpendicular to the eigenvector of the minimum eigenvalue (e_α), and the eddies experience the strong compression in that direction. Most of the coherent fine scale eddies experience weak stretching corresponding to the intermediate eigenvalue with the misalignment of about 15–17° with respect to the axial direction of the fine scale eddies. In the direction perpendicular to the (e_α, e_β) plane, the coherent fine scale eddies are significantly stretched by the maximum eigenvalue. These features do not depend on Reynolds number.

5. Spatial distributions of central axes of the coherent fine scale eddies

To investigate spatial distribution of the coherent fine scale eddies, the central axes of the fine scale eddies were identified by using axis tracing method (Tanahashi et al., 1999d). The axis tracing is conducted by following steps:

- From the point which was determined by the procedure of the vortex identification scheme, the point is moved in the axial direction by a short distance ***ds***. ***ds*** is parallel to the vorticity vector.
- Near the newly investigated point, a point that has minimum variance of azimuthal velocity is searched by the same procedure as described before.
- After the calculation of statistical properties, the above steps are repeated until minimum variance point cannot be found.

Fig. 12 shows spatial distributions of central axes of the coherent fine scale eddies for $Re_\tau = 800$. Spatial distributions of the axes in Fig. 12 show that the coherent fine scale eddies exist not only in the near-wall region but also in the whole flow field. Moreover, it is worth noting that central axes of the coherent fine scale eddies are distributed in viscous sub-layer for all three Re_τ cases, and axis positions nearest to the wall are about $y^+ = 0.6$, 0.8 and 0.9 for $Re_\tau = 180$, 400 and 800, respectively.

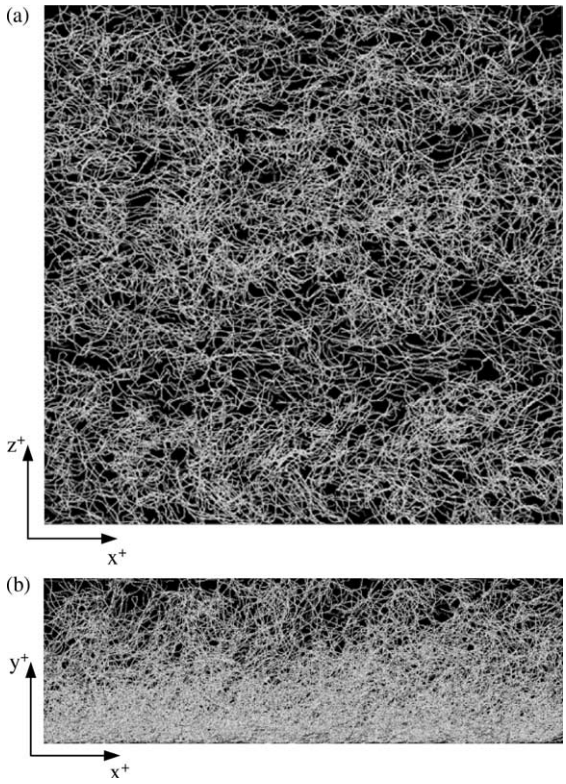

Fig. 12. Spatial distributions of central axes of the coherent fine scale eddies for $Re_\tau = 800$ (domain size: $l_x^+ \times l_y^+ \times l_z^+ = 2513 \times 800 \times 2513$): (a) top view, (b) side view.

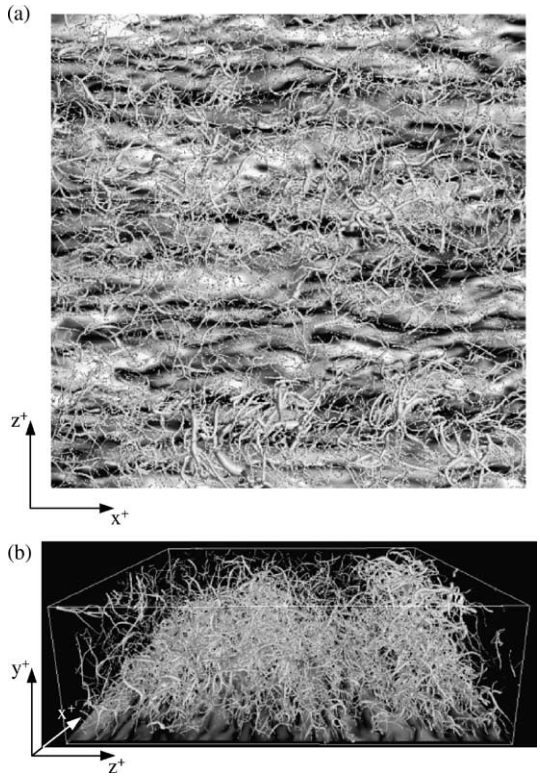

Fig. 13. Spatial distributions of central axes of the coherent fine scale eddies with contour of the instantaneous streamwise velocity fluctuation at $y^+ = 20$ for $Re_\tau = 800$ (domain size: $l_x^+ \times l_y^+ \times l_z^+ = 2513 \times 800 \times 2513$). Diameter of axis was drawn to be proportional to $\sqrt{Q^*}$. (a) Top view, (b) perspective view from the upstream.

Fig. 13 shows spatial distributions of the axes of the coherent fine scale eddies with contour of the instantaneous streamwise velocity at $y^+ = 20$ for $Re_\tau = 800$. In contour of the streamwise velocity, light-gray and dark-gray indicate high- and low-speed regions, respectively. Diameter of a central axis was drawn to be proportional to $\sqrt{Q^*}$ on the axes and Q^* is normalized by η and u_k. Therefore, wider axes possess stronger rotation rate. It is observed that the large clusters of central axes of the coherent fine scale eddies appear with a spanwise spacing of about 1100–1200 wall units. To inspect relation between the axes of the coherent fine scale eddies and high- and low-speed regions in more detail, the y^+ dependence of distributions of axes is shown in Fig. 14. In Fig. 14(a), it is clearly observed that central axes in low-speed streaks possess the relatively strong rotation rate near the wall. The distributions of the eddies with weaker rotation rate are not so related to low-speed streaks. These tendencies are hardly dependent on the wall-normal direction, but the lateral spacing between low-speed regions becomes wider leaving from the wall as shown in Fig. 14(b). These results suggest that low-speed streaks possess relatively larger second invariant of the velocity gradient tensor, which is closely related to fine scale eddies possessing the stronger rotation rate.

To estimate relation between the streak structure and the rotation rate of the coherent fine scale eddies quantitatively, conditional pdfs of the instantaneous streamwise velocity on the central axes of the coherent fine scale eddies are plotted in Fig. 15. The triangle and the rectangle symbols indicate pdfs conditioned by $Q^* > 1.05$ and $Q^* < 1.05$, respectively. For comparison, pdf of u'^+ without the condition is plotted. Here, the conditional value ($Q^* = 1.05$) is the average value of Q^* on central axes of the coherent fine scale eddies. The pdf of u'^+ for $Q^* > 1.05$ indicates that the probability in the low-speed regions is higher than that in the high-speed regions. The percentages of axis in the low-speed regions are 53.5% for all axes, 66.0% for $Q^* > 1.05$ and 48.7% for $Q^* < 1.05$.

To investigate structures of the fine scale eddies in details, spatial distributions of central axes in a typical domain are magnified in Fig. 16. The visualized region is $x^+ = 0$–2513, $y^+ = 0$–800 and $z^+ = 785$–1113, and the visualization method is the same as in Fig. 13. It is clearly observed that hairpin-like eddies and their packets (Adrian et al., 2000; Christensen and Adrian, 2001) exist in labeled zones I, II and III. Moreover, the two large clusters involving the packets of hairpin-like vortices are extended like mountains in the streamwise

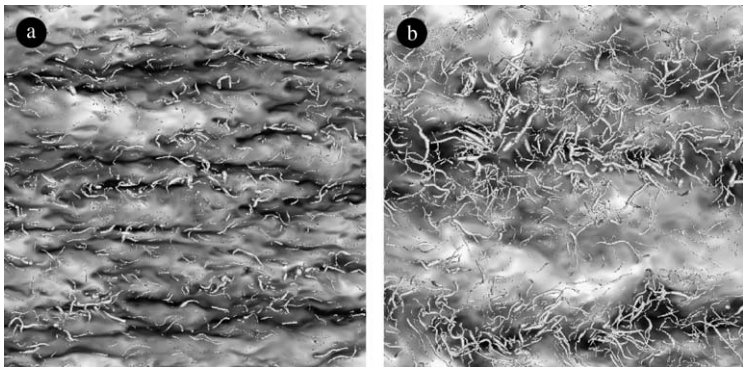

Fig. 14. The y^+ dependence of the distribution of axis of the coherent fine scale eddies ($Re_\tau = 800$, top view, domain size: $l_x^+ \times l_z^+ = 2513 \times 2513$). (a) $l_y^+ = 39$–60, u'^+ contour at $y^+ = 40$, (b) $l_y^+ = 199$–400, u'^+ contour at $y^+ = 200$.

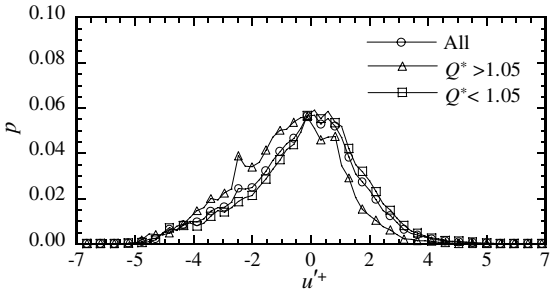

Fig. 15. The probability density function of the instantaneous streamwise velocity on the central axes of the coherent fine scale eddies ($Re_\tau = 800$).

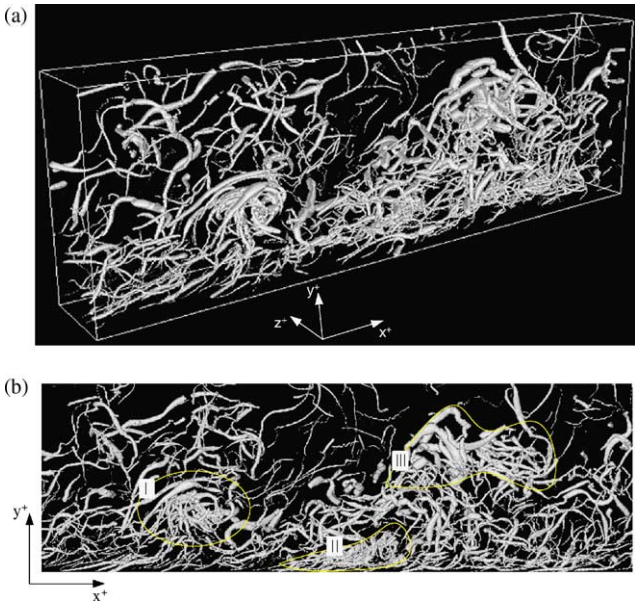

Fig. 16. Spatial distributions of central axes of the coherent fine scale eddies for $Re_\tau = 800$. Diameter of axis was drawn to be proportional to $\sqrt{Q^*}$ (domain size: $l_x^+ \times l_y^+ \times l_z^+ = 2513 \times 800 \times 328$). (a) Perspective view from above and upstream, (b) side view.

direction (see II and III regions). The hairpin-like vortices are one kinds of the coherent fine scale eddies, and their clusters or packets make further large structure.

6. Conclusions

In the present study, DNSs of turbulent channel flows were carried out up to $Re_\tau = 800$ to investigate the scaling law of fine scale eddies and their spatial distribution. To bring out fine scale eddies without any threshold, a new identification scheme based on local flow pattern was employed. The detected coherent fine scale eddies in turbulent channel flow can be scaled by the Kolmogorov microscale and the Kolmogorov velocity. In the near-wall region, the most expected diameter and maximum azimuthal velocity are about 10 times of the Kolmogorov microscale and 2.0 times of the Kolmogorov velocity, but become about 8 times of the Kolmogorov microscale and 1.2 times of the Kolmogorov velocity leaving from the wall. These results do not depend on Reynolds number. The inclination angles and the tilting angles of the rotating axes of fine scale eddies show strong directional dependence with decrease of y^+. These features correspond to streamwise vortices and hairpin-like vortices observed near the wall. In the case of $Re_\tau = 800$, the directional dependence of the rotating axis is observed even for $y^+ \approx 600$.

Strain rate acting on the coherent fine scale eddies can be scaled by the Kolmogorov microscale and the Kolmogorov velocity. The most expected eigenvalue ratio is $\alpha{:}\beta{:}\gamma = -7{:}1{:}6$ near the wall, but it becomes $\alpha{:}\beta{:}\gamma = -5{:}1{:}4$ to $-4{:}1{:}3$ leaving from the wall. It is indicated that the large compression and stretching are acting on the rotating plane of the coherent fine scale eddies near the wall. The eigenvector of the minimum eigenvalue has a tendency to be perpendicular to the axis of the coherent fine scale eddy and the most expected

angles between the axis and eigenvector of the intermediate eigenvalue are about 15–17°.

Central axes of the coherent fine scale eddies are distributed even in the viscous sub-layer. They form the large clusters with a spanwise spacing of about 1100–1200 wall units far from the wall ($y^+ \approx 400$). Relation between the instantaneous streamwise velocity and central axes shows that the stronger coherent fine scale eddies tend to exist in low-speed regions. Spatial distributions of central axes also show that hairpin-like vortex is a kind of the coherent fine scale eddies. In addition, the packets of hairpin-like vortices can form further large structure.

References

Adrian, R.J., Meinhart, C.D., Tomkins, C.D., 2000. Vortex organization in the outer region of the turbulent boundary layer. J. Fluid Mech. 422, 1–54.

Blackburn, H.M., Mansour, N.N., Cantwell, B.J., 1996. Topology of fine-scale motions in turbulent channel flow. J. Fluid Mech. 310, 269–292.

Brown, G.L., Roshko, A., 1974. On density effects and large structure in turbulent mixing layers. J. Fluid Mech. 64, 775–816.

Choi, H., Moin, P., Kim, J., 1994. Active turbulence control for drag reduction in wall-bounded flows. J. Fluid Mech. 262, 75–110.

Christensen, K.T., Adrian, R.J., 2001. Statistical evidence of hairpin vortex packets in wall turbulence. J. Fluid Mech. 431, 433–443.

Corrsin, S., 1962. Turbulent dissipation fluctuations. Phys. Fluids 10, 1301–1302.

Jeong, J., Hussain, F., Schoppa, W., Kim, J., 1997. Coherent structures near the wall in a turbulent channel flow. J. Fluid Mech. 332, 185–214.

Jimenez, J., Wray, A.A., Saffman, P.G., Rogallo, R.S., 1993. The structure of intense vorticity in isotropic turbulence. J. Fluid Mech. 255, 65–90.

Kim, J., Moin, P., Moser, R.D., 1987. Turbulence statistics in fully developed channel flow at low Reynolds number. J. Fluid Mech. 177, 133–166.

Kim, J., 1983. On the structure of wall-bounded turbulent flows. Phys. Fluids 26, 2088–2097.

Lundgren, T.S., 1982. Strained spiral vortex model for turbulent fine structure. Phys. Fluids 25, 2193–2203.

Miyauchi, T., Tanahashi, M., Iwase, S., 2002. Coherent fine scale eddies and energy dissipation rate in homogeneous isotropic turbulence up to $Re_\lambda \approx 220$, presented at IUTAM symposium on Reynolds number scaling in turbulent flow.

Moser, R.D., Kim, J., Mansour, N.N., 1999. Direct numerical simulation of turbulent channel flow up to $Re_\tau = 590$. Phys. Fluids 11, 943–945.

Pullin, D.I., Saffiman, P.G., 1993. On the Lundgren–Townsend model of turbulent fine scales. Phys. Fluids A 5, 126–145.

She, Z.S., Jackson, E., Orszag, S.A., 1990. Intermittent vortex structures in homogeneous isotropic turbulence. Nature 344, 226–228.

Soldati, A., 2000. Modulation of turbulent boundary layer by EHD flows. ERCOFTAC Bull. 44, 50–56.

Tanahashi, M., Iwase, S., Miyauchi, T., 2001. Appearance and alignment with strain rate of coherent fine scale eddies in turbulent mixing layer. J. Turbul. 2, 17 pp.

Tanahashi, M., Miyauchi, T., Ikeda, J., 1999a. Identification of coherent fine scale structure in turbulence. Simul. Ident. Organized Struct. Flow, 131–140.

Tanahashi, M., Das, S.K., Shoji, K., Miyauchi, T., 1999b. Coherent fine scale structures in turbulent channel flows. Trans. JSME 65, 3244–3251.

Tanahashi, M., Shiokawa, S., Das, S.K., Miyauchi, T., 1999c. Scaling of fine scale eddies in near-wall turbulence. J. Jpn. Soc. Fluid Mech. 18, 256–261.

Tanahashi, M., Iwase, S., Uddin, Md.A., Miyauchi, T., 1999d. Three-dimensional features of coherent fine scale eddies in turbulence. In: Proc. 1st Int. Symp. Turbulence and Shear Flow Phenomena. Begell House, pp. 79–84.

Tanaka, M., Kida, S., 1993. Characterization of vortex tubes and sheets. Phys. Fluids A 5, 2079–2082.

Tennekes, H., 1968. Simple model for the small-scale structure of turbulence. Phys. Fluids 11, 669–761.

Townsend, A.A., 1951. On the fine-scale structure of turbulence. Proc. Royal Soc., Lond. A 208, 534–542.

Zhou, J., Adrian, R.J., Balachandar, S., Kendall, T.M., 1999. Mechanisms for generating coherent packets of hairpin vortices in channel flow. J. Fluid Mech. 387, 353–396.